CHEMISTRY OF MATERIALS

Article

pubs.acs.org/cm

Ultrafast Formation of Free-Standing 2D Carbon Nanotube Thin Films through Capillary Force Driving Compression on an Air/Water Interface

Peng Xiao,[†] Jincui Gu,[†] Changjin Wan,[†] Shuai Wang,[†] Jiang He,[†] Jiawei Zhang,*[,†] Youju Huang,[†] Shiao-Wei Kuo,[‡] and Tao Chen*[,†]

[†]Ningbo Institute of Material Technology and Engineering, Key Laboratory of Graphene Technologies and Applications of Zhejiang Province, Chinese Academy of Science, Zhongguan West Road 1219, 315201, Ningbo, Zhejiang, China

[‡]Department of Material and Optoelectronic Science, National Sun Yat-Sen University, 804, Kaohsiung, Taiwan

Supporting Information

ABSTRACT: The Langmuir–Blodgett (LB) technique has been demonstrated as the most popular way to achieve freestanding two-dimensional (2D) carbon nanotubes (CNTs) thin films on the surface of liquid, yet still suffers some limitations, such as the need of expensive instruments with complicated surface pressure detection and time-consuming processes, and thus is inaccessible to a large number of researchers. Here, we present a cheap, reliable, and ultrafast strategy to fabricate free-standing 2D CNTs networks on an air/water interface by a highly simplified LB method free of instruments, yet only with porous materials assisted capillary force driving compression. The formation of free-standing 2D CNTs networks with controlled thickness, transmittance, and conductivity could be further transferred to other various substrates. Growing polymer from one side of the flexible CNTs network allows us to achieve 2D hybrid Janus materials of polymer grafted CNTs thin films. This endows the conductive 2D CNTs hybrid networks with responsive chemical functionality, which is highly important for scalable developments as next generation flexible electronics in chemical sensing.

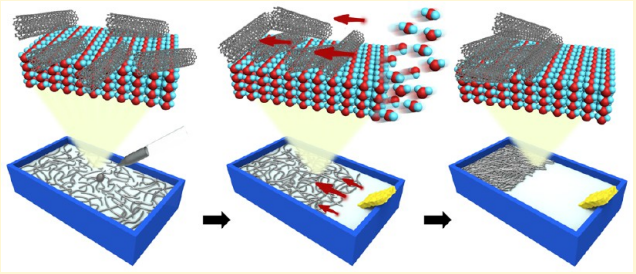

1. INTRODUCTION

Transparent and conductive two-dimensional (2D) carbon nanotubes (CNTs)[1] thin films have received considerable interest due to their unique properties, such as high porosity and specific surface area, high optical transmittance, high thermal conductivity and chemical sensitivity, good mechanical flexibility, and tunable semiconducting properties,[2−8] which open a new avenue for a wide range of applications. 2D CNTs thin films are suitable for further integration into novel flexible electronic devices.[9−11] It is known that much effort has been made to achieve 2D CNTs thin film generally by either chemical vapor deposition (CVD) growth approaches or suspension-based deposition methods.[7] Due to the harsh requirements of CVD growth for high temperature, there are so many challenges to limit their unique applications for flexible electronic devices.[4,5,12] Alternatively, 2D CNTs thin films could be formed by various wet processes including dip-coating,[13] spin-coating,[14] spray-coating,[11] layer-by-layer assembly (LBL),[15,16] filtration assembly,[3,5,17,18] and the Langmuir–Blodgett (LB) technique.[19−22] Among these strategies, the LB method has been demonstrated as the most popular way to achieve free-standing 2D CNTs thin films on the surface of liquid,[20,23] which may open up new opportunities for further asymmetrical 2D chemistry[24−26] in many applications since they could be easily transferred to various targeted substrates. Although attractive, the LB process still suffers some limitations, including the need of expensive and specialized apparatus, large spaces, and the complicated surface pressure detection process[23] and thus is inaccessible to a large number of researchers. Therefore, more simple, cheap, and reliable LB approaches for fabricating free-standing 2D CNTs thin films are still highly required.

Herein, we reported a robust strategy with low cost to fabricate free-standing 2D CNTs thin film networks on an air/water interface by a highly simplified LB method without the need of expensive instruments and surface pressure detection, yet only with porous materials assisted capillary force induced compression. Our strategy as a significant advancement of the LB technique is thus accessible to a great deal of researchers and has the potential as a general approach to achieve Langmuir film of various nanomaterials on the surface of water. The formation of resulting free-standing 2D CNTs networks with controlled thickness, transmittance, and conductivity on the interface allows the further transfer to other substrates. In order to realize the full potential of 2D CNTs thin films, defined chemical functionality on CNTs films by growing

Received: August 16, 2016
Revised: September 17, 2016
Published: September 18, 2016

DOI: 10.1021/acs.chemmater.6b03420
Chem. Mater. 2016, 28, 7125−7133

Scheme 1. Schematic Illustration of Macroscopical Self-Assembly of Free-Standing, Transparent, and Conductive 2D CNTs Films on an Air/Water Interface Driven by Porous Materials Assisted Capillary Force Induced Compression

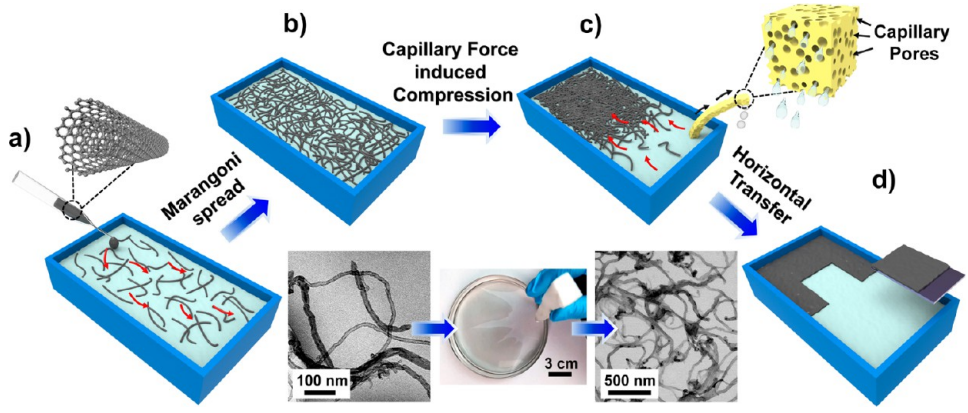

[a](a) Injection of CNTs ethanol dispersions spreading onto the surface of water. (b) The well-dispersed CNTs film in a loosely compacted state floats on the surface of water. (c) A porous sponge assisted capillary force driven compression process for a closely packed CNTs film. (d) A closely compacted state of the free-standing 2D CNTs thin film could be transferred to any other various target substrates.

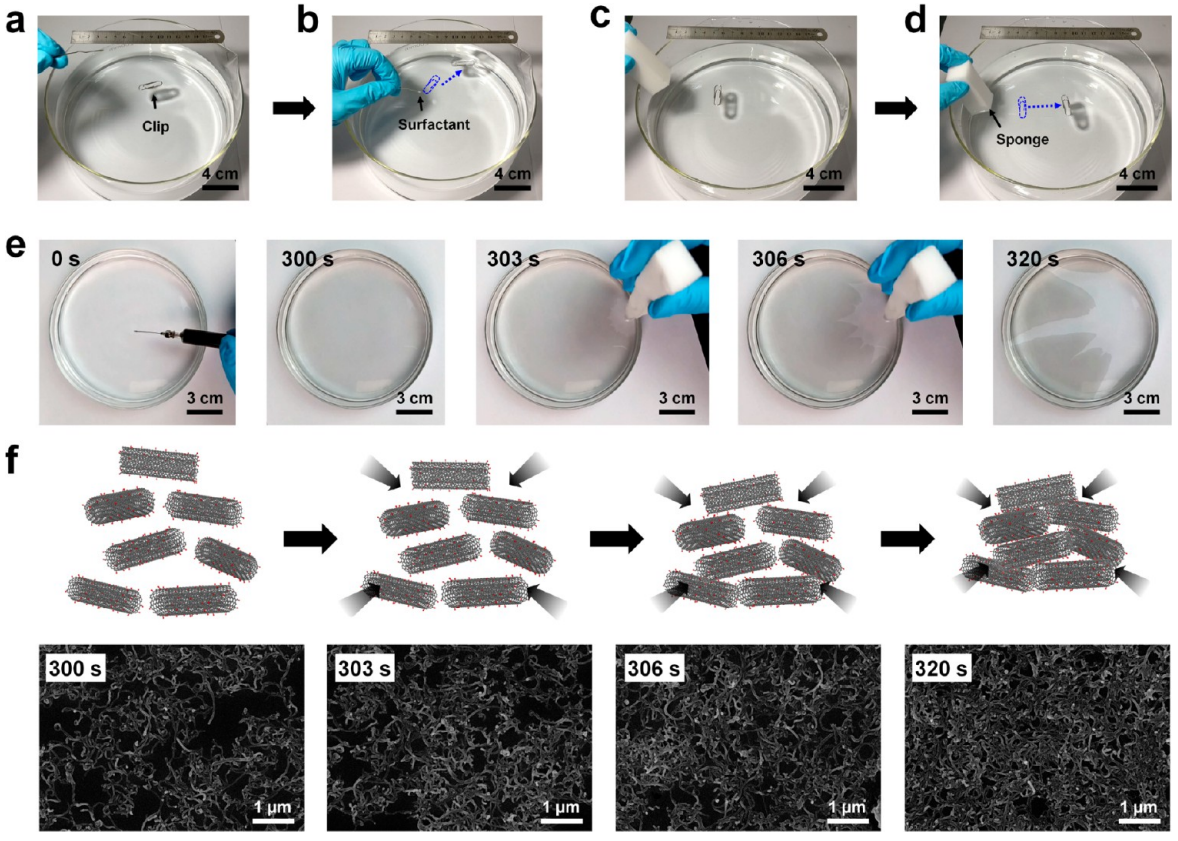

Figure 1. (a, b) Photos of the clip motion driven by the surfactant induced surface tension difference between the two sides of the clip. (c, d) Photographs of the commercial porous sponge induced by the clip motion based on the surface tension difference. (e) Photos of the process of fabricating free-standing 2D CNTs thin films, including the injection of CNTs dispersion onto the surface of water and the compression process of CNTs with a loosely compacted state by a commercial porous sponge. (f) SEM images of the free-standing CNTs networks in a various density with increasing compression time.

responsive polymer from one side was also developed. Our strategy thus allows us to achieve 2D hybrid Janus materials of polymer grafted CNTs thin films and endows the conductive CNTs networks with responsive chemical functionality, which is highly important for scalable and low cost developments as a next generation of flexible electronics such as in chemical sensing.

2. RESULTS AND DISCUSSION

The fabrication process of free-standing, transparent, and conductive 2D CNTs thin films on the surface of water driven by porous materials assisted capillary force induced compression is schematically illustrated in Scheme 1. When the CNTs dispersion in ethanol was injected onto the surface of water (Scheme 1a), they were rapidly pushed outward from ethanol-

DOI: 10.1021/acs.chemmater.6b03420
Chem. Mater. 2016, 28, 7125−7133

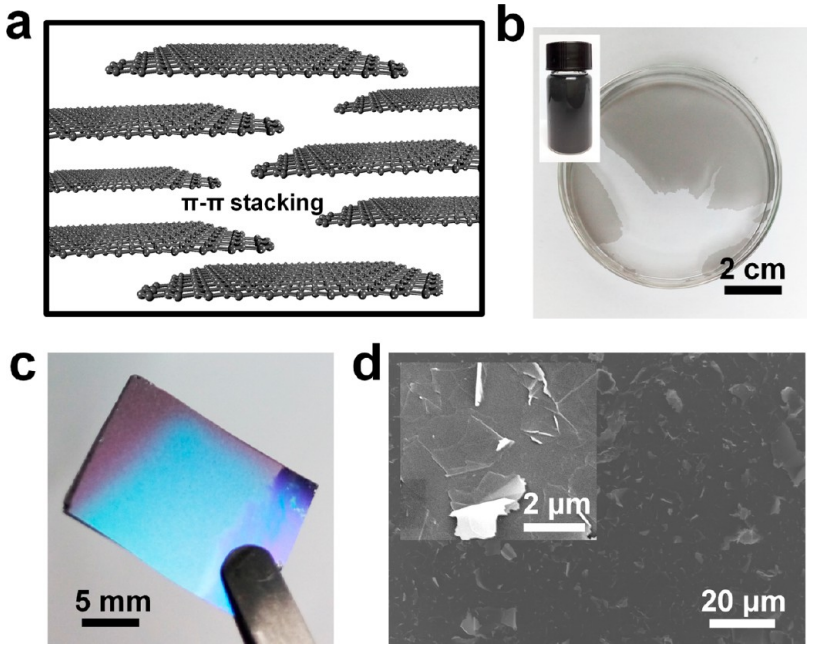

Figure 2. (a) Schematic illustration of graphene sheets closely packed into an integral film through $\pi-\pi$ stacking interaction. (b) Photograph of graphene film. Inset: ethanol-assisted graphene dispersion. (c) Photo of graphene film transferred onto the SiO_2 substrate. (d) SEM images of the graphene film with closely packed structures. Inset: the enlarged image of the graphene film.

rich regions with low surface tension to water-rich regions with high surface tension owing to the strong Marangoni forces.[27] The homogeneous CNTs Langmuir thin film with a loosely compacted state was then formed at the air/water interface (Scheme 1b). Different from the typical LB method for fabricating close packed monolayer films induced by a moving barrier with surface pressure detection,[20] a porous sponge with abundant capillary pores was used to siphon one side of the water surface. This could induce the motion of CNTs quickly on the surface of water to the opposite direction (Scheme 1c). A close compacted state of the free-standing 2D CNTs thin film was finally achieved and could be transferred to any other various target substrates (Scheme 1d).

As an attractive method for fabricating well-defined layered structures on liquid substrate, the LB strategy can be employed to achieve free-standing 2D CNTs thin films on the surface of an aqueous subphase in a shallow Langmuir trough that must equipped with Teflon barriers to compress CNTs for a formation of CNTs monolayers.[28] During this process, surface pressure changes of the monolayer need be monitored *in situ* using a Wilhelmy-type surface balance. Despite being appealing, the requirement of the LB instrument and detection procedure makes it inaccessible to general researchers. We have known that surface tension is a powerful tool that can drive small objects, such as clip, leaves, etc., floating on the surface of liquid to move along one direction upon the change of surface tension. This can be controlled by the addition of a drop of surfactant onto one side of the clip (Figure 1a,b and Movie S1). The motion of the floating clip could also be achieved effectively when we use the commercial porous water absorbent materials, such as a sponge, to induce the change of surface tension via the capillary force created during the absorption of water with the sponge (Figure 1c,d and Movie S2). Thus, it is believed that the capillary force driven motion behavior can be extended to the micro- and even nanoscale system to induce the compression of floating CNTs dispersions on the surface of water.

The whole injection process of CNTs ethanol dispersion onto the surface of water and subsequent compression process of CNTs was monitored by optical images. As displayed in Figure 1e and Movie S3, with the appropriate injection volume of CNTs dispersion, the surface of water was fully covered with the CNTs Langmuir monolayers that were driven by the Marangoni effects.[27,29] When the porous sponge was put inside the CNTs covered water, the floating CNTs immediately experienced a spontaneous compression toward the opposite side of the water absorption direction. It is noted that with the increase of the immersion time of the sponge, the area of the assembled CNTs thin film continually contracted to a saturated point within 20 s. Since interactions among CNTs are dynamically balanced, further water absorption could not drive the CNTs with further movement again. This porous materials assisted capillary force induced compression of CNTs thin films was also confirmed via the microscopic structures of free-standing networks investigated by SEM (Figure 1f), which showed a more close compacted state with the increase of time.

Furthermore, this facile strategy could be further extended to a variety of nanomaterials to form close-packed films at the air/water interface. As a proof of concept, physical exfoliated graphene sheets were employed to explore the universality of this method. As displayed in Figure 2a,b, the preassembled graphene film can be effectively compressed using the sponge and ultimately achieve a stable morphology owing to the strong $\pi-\pi$ stacking interaction among graphene sheets. Moreover, the as-prepared film can be further transferred onto the silicon surface without any fracture (Figure 2c). The transferred film has demonstrated uniform microstructure with closely compacted graphene sheets (Figure 2d). Additionally, reduced graphene oxide (RGO) nanosheets and SiO_2 nanoparticles were also chosen to form free-standing thin films upon the

DOI: 10.1021/acs.chemmater.6b03420
Chem. Mater. 2016, 28, 7125−7133

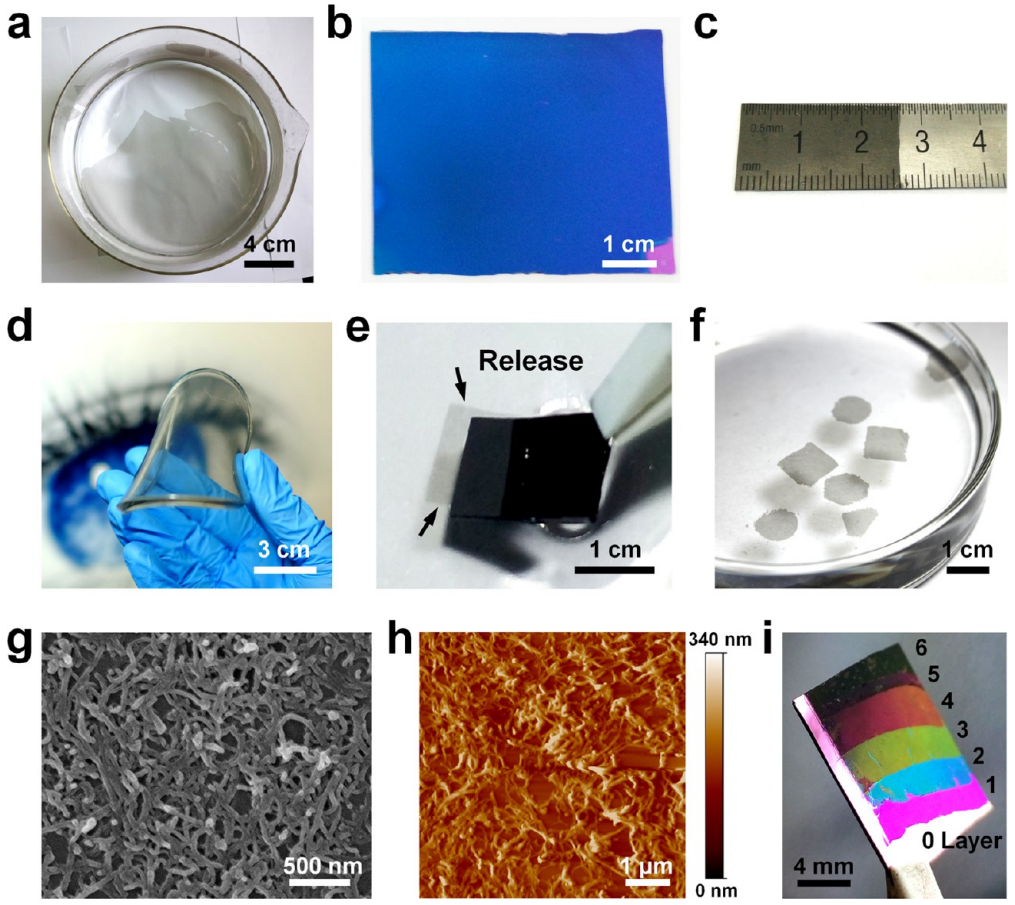

Figure 3. (a) CNTs thin film assembled on the surface of the water in a large area. (b) Transparent and homogeneous CNTs thin film transferred onto the silicon surface. (c) Photograph of the transferred CNTs thin film on a steel ruler. (d) Optical images of CNTs thin film transferred to a flexible PDMS substrate. (e) Photograph of the transferred CNTs thin film subsequently transferred onto another surface of the water. (f) Photos of various shaped CNTs films floating on the surface of water. (g) SEM image of the homogeneous CNTs thin film transferred onto silica wafer. (h) AFM image of the homogeneous CNTs thin film transferred onto silica wafer. (i) Photo of the multitransfer of the CNTs thin film with a dramatic color change due to the multilayer structures at a certain viewing angle under the blue violet SiO_2 background.

driving by a porous materials induced compression (see Figures S1 and S2).

As an efficient method to fabricate free-standing, transparent, and conductive 2D CNTs films on the surface of water, our simple and robust strategy could be used to fabricate the macroscopical preparation of CNTs network in a large scale. The optical photograph of a typical free-standing and transparent CNTs thin film on the surface of water is shown in Figure 3a. With strong intertube connections, the film is able to maintain the closely packed state even when the sponge is withdrawn. The advantage of free-standing CNTs thin films assembled on the surface of the solution may open new opportunities for various applications since they can be easily transferred to an arbitrary substrate such as silicon, coins, polydimethylsiloxane (PDMS), etc. for the integration into flexible devices. Figure 3b shows the photograph of blue-colored film on a flat SiO_2 background in high-uniformity. Metal surfaces, such as a steel ruler and embossed metal, are also employed to support the CNTs film, which can still maintain a continuous state (Figures 3c and S3). Moreover, a flexible PDMS could also be used as the supported substrate, presenting potential applications in wearable electronics (Figure 3d). It is more interesting that the floating CNTs thin films could be further released onto another surface of liquid after previous transfer on the SiO_2 surface (Figure 3e), which allows the further interfacial reaction from the water facing side.[30] Surprisingly, the shape of the released 2D CNTs thin film could be specifically designed into various geometries such as circular, square, triangular, and hexagonal at the air/water interface upon the change of substrate shape (Figure 3f). The morphology of the as-prepared CNTs thin film on a silicon wafer was characterized by SEM and AFM, which showed that the substrate is covered with a porous and mesh-like network of entangled CNTs with random oriented individual CNTs (Figure 3g,h). A Raman spectrum was also conducted to explore the structural information with remarkable characteristic peaks of D, G, and 2D bands (see Figure S4). More interesting, the transferred CNTs thin film could also be used as the supported substrate for a subsequent multitransfer just like the LBL strategy for desired thickness. Due to the multilayer related thickness variation, colorful transition could be adjusted from purple to black at a certain viewing angle under the white light (Figure 3i), which has potential application in flexible display devices.

The thickness and corresponding transmittance of free-standing 2D CNTs thin films could be controlled by changing the concentrations of CNTs dispersions. When CNTs dispersions were injected on the water surface, owing to the strong Marangoni effect, the ethanol with CNTs moved quickly toward the high surface tension area (water-rich). In this

DOI: 10.1021/acs.chemmater.6b03420
Chem. Mater. 2016, 28, 7125−7133

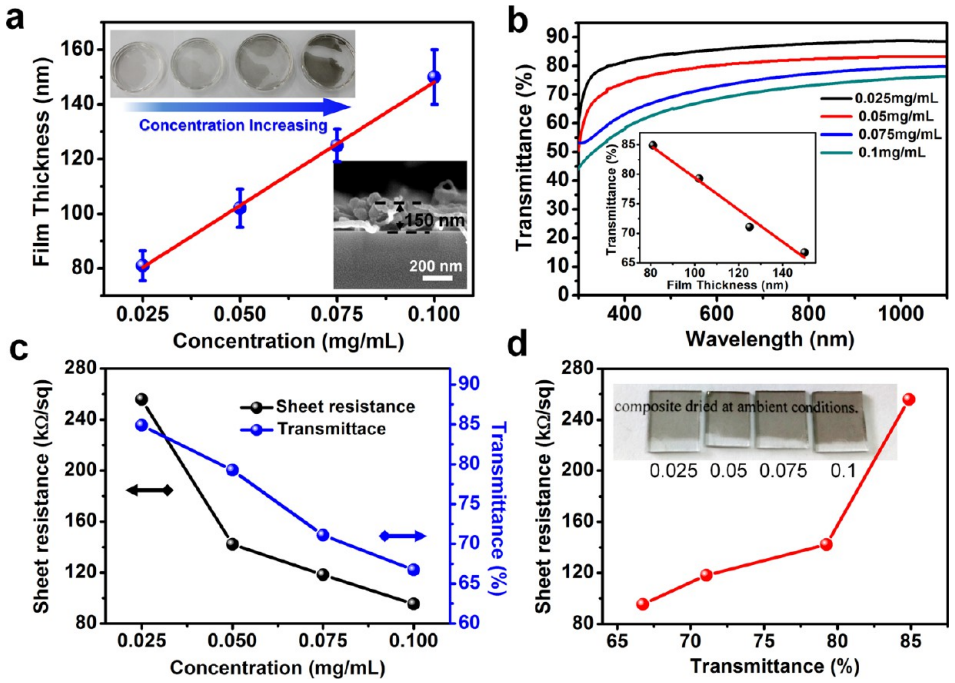

Figure 4. (a) Film thickness versus concentration curve of CNTs films. Inset: photographs of assembled CNTs thin film on the surface of water by using dispersion concentration and SEM image of the cross-section of the CNTs thin film. (b) Transmittance of CNTs thin films assembled by different concentrations. Inset: The curve of transmittance vs film thickness. (c) Sheet resistance vs concentration and transmittance vs concentration curves of CNTs thin films. (d) Sheet resistance vs transmittance curve. Inset: Photos of assembled CNTs films fabricated by different original dispersion concentrations transferred onto glass substrates.

process, CNTs would collide randomly and bind together. Higher CNTs suspension concentration results in a greater collision rate to form a thicker layer. With the concentration increasing from 0.025 to 0.1 mg/mL, the thickness has a prominently linear dependence from 81 to 150 nm (Figure 4a) that is confirmed by AFM and/or SEM. More importantly, different CNTs dispersion concentration used to fabricate thin films also resulted in striking changes in the optical and electronic properties. The transmittance spectra of the thin film were carried out by a UV−vis-near IR spectrophotometer. Figure 4b shows the transmittance of CNTs films fabricated by different original CNTs dispersion concentrations, presenting that a transmittance at 550 nm has a decreasing trend ranging from 84.9% to 66.7% and a good linear relationship with the thickness of the films (Inset in Figure 4b). As displayed in Figure 4c, with the increase of concentration of the CNTs dispersions, the average value of the sheet resistance demonstrates a decrease from 255.8 to 95.4 kΩ/sq, respectively, as well as that of the transmittance. Moreover, Figure 4d summarizes the sheet resistance vs transmittance of the thin film made from various original concentrations of CNTs dispersion, which showed a linear increase of sheet resistance along the transmittance. Importantly, compared with previously reported works,[31,32] the CNTs films with only 3 to 5 layers randomly stacked show comparative conductivity, which represent potential applications in flexible electronic skin and sensing devices.

Named after the two-faced Roman God Janus, the term of Janus has thus been used to describe materials having different properties at opposite sides, which thus have attracted tremendous attention in various applications.[33,34] Among the Janus materials,[26,35] the realization of 2D Janus sheets, membranes, or thin films still remains a significant challenge and has not been developed sufficiently so far. The transferred 2D CNTs thin film on silica wafer with full protection of the contacted side of CNTs thin film with substrates provides the potential asymmetric surface modification for achieving free-standing large-sized self-supporting 2D Janus thin films.[36] Photoactive HO^- groups on CNTs could be initiated to grow responsive polymer,[37−39] such as poly(*N*,*N*-dimethylaminoethyl methacrylate) (PDMAEMA), by SIPGP from CNTs thin film, which allows the fabrication of the 2D Janus hybrid thin film in a simple strategy (Figure 5a). After polymerization, SEM characterization was conducted to explore the morphology information on both sides of the resulting hybrid. Compared with the smooth morphology of the top layer that was fully covered with polymer with almost no CNTs visible, the presence of the abundant bare CNTs of the bottom layer strongly evidenced the Janus structure (see Figure S5). Furthermore, the conductivity difference was also characterized, demonstrating an asymmetric structure with an insulative top layer and a conductive bottom layer (see Figure S6). The obtained 2D Janus hybrid endows the CNTs networks with responsive chemical functionality and maintains competent conductivity, which is highly important for scalable and low cost developments as next generation flexible electronics in chemical sensing. As shown in Figure 5b, a free-standing 2D Janus material of PDMAEMA grafted CNTs thin film could be achieved after the etching process and then could be retransferred onto Au electrodes as a flexible device of field-effect transistor (FET). Compared with pure CNTs thin film FET, PDMAEMA grafted CNTs thin film FET demonstrates a remarkable higher current on−off ratio (I_{ON}/I_{OFF}) of ∼2.5 order of magnitude (Figure 5c).

Since PDMAEMA has some tert-ammonia groups in the main chain, the PDMAEMA grafted CNTs thin films FET

DOI: 10.1021/acs.chemmater.6b03420
Chem. Mater. 2016, 28, 7125−7133

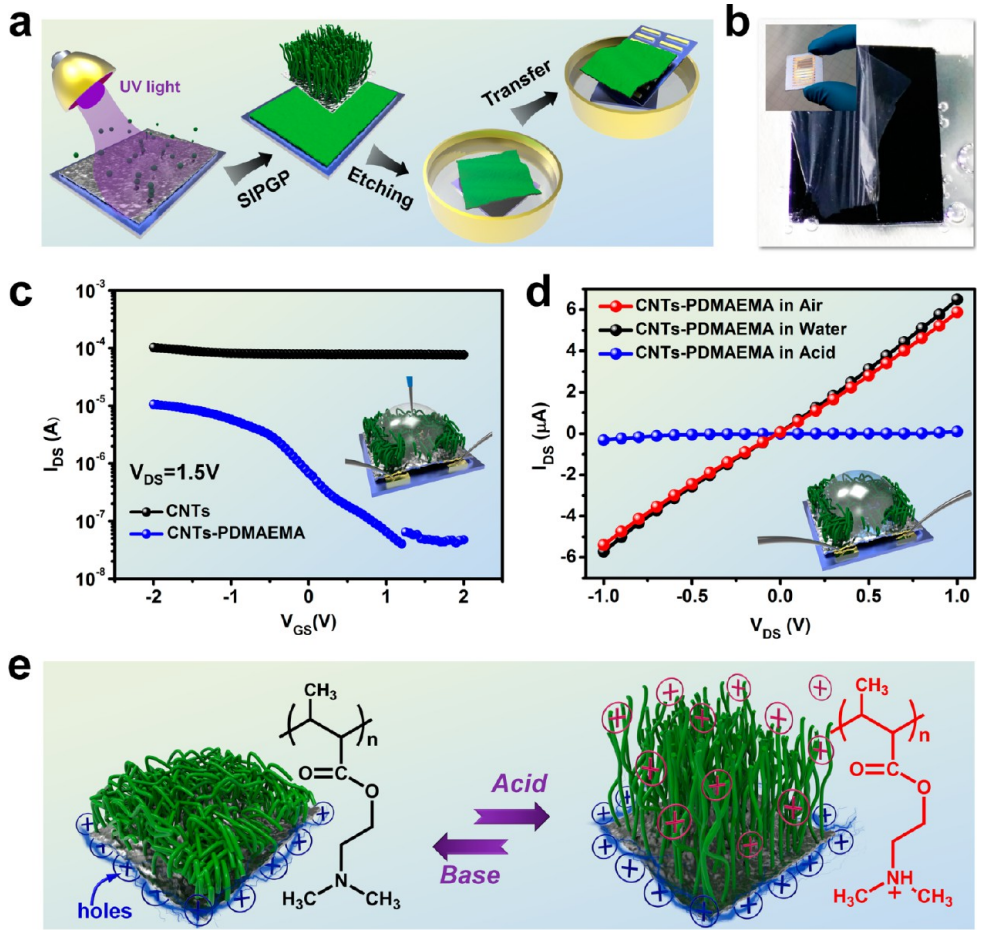

Figure 5. (a) Schematic process of polymerization, etching, and transfer of the PDMAEMA brush functionalized CNTs thin film onto patterned Au electrodes. (b) Photograph of the process of etching the film, indicating flexible and transparent properties. Inset: the hybrid transferred onto the Au electrodes surface. (c) FET transfer characteristics of bare CNTs vs PDMAEMA grafted CNTs. (d) Current−voltage curves of PDMAEMA brush functionalized CNTs responses in air, water, and acid solution, respectively. (e) The possible mechanism of the transition process of PDMAEMA protonation induced by acid solution.

could thus be used as the chemical sensor for the response of pH. Figure 5d showed the $I-V$ curves at the voltage range of −1.0 to 1.0 V. As expected, compared with the dry-state hybrid, the wet-state one in deionized water (pH = 8.1) only showed a slight increase of the conductivity. However, when exposed to acid (pH = 3.5), the current ratio (I_{water}/I_{acid}) at V_{DS} = 1.0 V is estimated to be approximately 66.3. The potential mechanism of pH-sensitive CNTs-PDMAEMA hybrid network is illustrated in Figure 5e. After exposure to acid solution, the PDMAEMA brush experiences a phase transition, as well as charge transition behavior from collapsed conformation and electrically neutrality to stretched conformation with amounts of positive charges.[40,41] The positive charges, which are abundantly present in the polymer/CNTs interface, can be analogous to the positive gate voltage effect on the CNTs. As the CNTs are a p-type semiconductor, the holes in the CNTs can be depleted by such positive gate voltage, which result in a dramatic decrease in conductance. Therefore, the cationic concentration can be reflected by the conductance of the CNTs due to such electrostatic modulation effect.

3. CONCLUSIONS

In summary, we have demonstrated a simple and cost-effective method to fabricate free-standing 2D CNTs thin films through a highly simplified LB method without the use of an expensive instrument and surface pressure detection procedure and only porous materials assisted capillary force optimized compression on the surface of water. It is a highly significant advancement of the LB technique with a green operation process and thus is accessible to general researchers and has the potential as a general strategy to achieve an efficient Langmuir film of various nanomaterials on the surface of water. The formation of the resulting free-standing 2D CNTs thin networks with controlled thickness, transmittance, and conductivity on the surface of water allows the further transfer to other substrates for various applications. Especially, through the alternative introduction of the stimuli-responsive polymer onto one side of the CNTs networks, a 2D Janus hybrid with multifunctionality can be achieved, which could be used to realize the full potential of the 2D hybrid materials by using the stimulus responsivity of the polymer to detect an external environment change, which could induce the conformation of polymer structure and then transform the information to CNTs thin film with electronic information output. This is a new advancement in demonstrating scalable developments as next generation electronic devices in chemical or biological sensors.

4. EXPERIMENTAL SECTION

Materials. The raw carbon nanotubes (CNTs) (diameter, about 10−30 nm; length, about 10−30 μm; −OH %, about 2 wt %%) with a

DOI: 10.1021/acs.chemmater.6b03420
Chem. Mater. 2016, 28, 7125−7133

purity of over 90% were acquired from Chengdu Organic Chemistry Co., Ltd., and were rinsed thoroughly with anhydrous ethanol and dried in a stream of nitrogen before use. General chemicals of chemical reagent grade were used as received from Sinopharm Chemical Reagent. Ethanol and deionized water were used as rinsing solvents. *N*,*N*-Dimethylaminoethyl methacrylate (DMAEMA) was obtained from Alfa Aesar China (Tianjin) Co., Ltd., which was purified by a neutral Al_2O_3 column and dried with a 0.4 nm molecular sieve at room temperature for 3 days. Silicon wafers were cleaned in a mixture of H_2O_2/H_2SO_4 (1:3, v/v) at 80 °C ("piranha solution") for 2 h and washed thoroughly with Milli-Q-grade water. *(Caution: Piranha solution reacts violently with organic matter!)*

Preparation of Electrochemical Exfoliated Few-Layer Graphene Flakes. Few-layer graphene flakes were exfoliated from graphite through the electrochemical exfoliation method. The lateral size of the exfoliated graphene is about 2−20 μm and the thickness is ∼4−5 nm.

Oxidation−Reduction Method for Reduced Graphene Oxide Nanosheets (RGO). GO sheets were synthesized by a modified Hummers' method[42] and exfoliation of graphite oxide was achieved by a strong ultrasonication method. The obtained brown dispersion was then washed and centrifuged to remove any unexfoliated graphite oxide. The GO suspension was cooled down to 0 °C in the ice bath, followed by the dropwise addition of 8 mM hydrazine solution. Subsequently, further reduction was carried out by heating the RGO suspension on a flat heater at 250 °C for 1 h.

Preparation of CNTs, Few-Layer Graphene, and RGO Dispersions. The carbon-based nanotubes or sheets were first dispersed in anhydrous ethanol solution, followed by strong ultrasonication for 2 h to form a stable dispersion with appropriate aging time.

Preparation of CNTs, Few-Layer Graphene, and RGO Film. The ethanol-assisted carbon materials dispersion was injected dropwise onto the water surface for appropriate volume. It is noted that it is necessary to employ a relatively slow drop speed to achieve a homogeneous spread. Importantly, when the injection volume reaches the saturation point, further injection may result in remarkable agglomeration at the injected location. As a result, after appropriate injection, uniform Langmuir monolayers were finally formed at the liquid/air interface. Subsequently, capillary substances like tissue or microporous sponges were selected to put on one side of the interface to quickly siphon water from the system, followed by a prominent decrease of the Langmuir area. Notably, the homogeneous Langmuir monolayers were closely packed toward the opposite direction of the siphone direction. When the movement of the film stopped and further siphoning could not drive the film, the resulting film was ultimately formed, indicating a closely packed structure.

Transfer of the As-Formed Films. In our system, the resulting film was transferred using the horizontal transfer method, followed by a N_2 drying procedure.

Self-Initiated Photografting and Photopolymerization (SIPGP). The silicon supported as-prepared CNTs film was submerged in ∼2 mL of distilled and degassed monomer and irradiated with an UV lamp with a spectral distribution between 300 and 400 nm (intensity maximum at λ = 365 nm with a total power of ∼240 mW/cm^2) for a required time of about 2 h. Following SIPGP,[43] the functionalized film was exhaustively rinsed with ethanol for several times to remove any physisorbed PDMAEMA.

Fabrication of Freestanding PDMAEMA Grafted Films. The polymer brushes grafted CNTs film was cleaved from the silicon surface by immersing the silicon wafer in NaOH solution (1 M). After several hours (usually 6−8 h), the film was easily released from the substrate. Due to the hydrophilic property of the grafted PDMAEMA brushes, the resulting film is flexible and tends to form a wrinkle in the water. In order to have a direct contact between the unmodified CNTs side of the hybrid and the Au electrodes, in our experiments, when the hybrid film was not completely released from the substrate, the substrate with patterned Au electrodes was used to transfer the film with an angle of inclination. Finally, the resulting film was exhaustively rinsed with deionized water for several times and dried in N_2 atmosphere. For FET fabrication, source-drain electrodes were patterned on glass substrates with two patterned Au films with a distance of about 60 μm and thickness about 30 nm by electron-beam evaporation. The etched 2D Janus hybrid was then deposited on the patterned Au electrodes surface, resulting in the bottom conductive layer being contacted tightly with the electrodes and the top polymer layer pointing toward the air. Deionized water was dropped on the surface of the top layer of the Janus for a water-gated FET configuration. For pH-solution sensing, the top polymer part of the device was exposed to 50 μL of the buffered pH (a phosphate buffer solution of pH = 3.5) solutions. For every cycle, the buffer solution was drawn away and then thoroughly rinsed with deionized water.

5. CHARACTERIZATION

Field emission scanning electron microscope (FE-SEM) images were obtained with a FE scanning electron microanalyzer (Hitachi-S4800, 4 kV). Transmission electron microscopy (TEM) was recorded by a transmission an electron microscope (JEM-2100F, accelerating voltage of 200 kV). TEM samples were prepared by dropping a diluted aqueous solution of CNTs onto carbon-coated copper grids and dried in air. Atomic force microscopy (AFM) images were taken by a multimode AFM (Being Nano-Instruments, Ltd.) operating in the contact and/or tapping mode using silicon cantilevers (spring constant: 0.15 N m^{-1}; resonant frequency: 12 kHz for the cantilever of contact mode; spring constant: 3−40 N m^{-1}; resonant frequency: 75−300 kHz for the cantilever of tapping mode). Optical transmittance of the films was probed using UV−vis−NIR spectra, which were obtained with a TU-1810 spectrophotometer from Beijing Purkinje General Instrument Co. Ltd. in transmission mode. Optical images were acquired by polarized optical microscopy (Olympus, BX 51TF Instec H601). The Raman scattering measurements were performed at room temperature on a Raman system (inVia-reflex, Renishaw) with confocal microscopy. The solid-state diode laser (532 nm) was used as an excitation source with a frequency range of 3200−1000 cm^{-1}. Electrical measurements of devices were performed with a semiconductor parameter analyzer (Keithley 4200). The volume resistance of the as-prepared CNTs films on SiO_2/Si surfaces were measured on a NAPSON CRES-BOX Semi-automatic four-point probe sheet resistance/resistivity measurement system. For each sample, 6 different points were measured and averaged.

■ ASSOCIATED CONTENT

Supporting Information

The Supporting Information is available free of charge on the ACS Publications website at DOI: 10.1021/acs.chemmater.6b03420.

Optical and AFM/SEM images of the reduced graphene oxide (RGO) and SiO_2 nanoparticles; Optical images of CNTs film transferred onto embossed metal surfaces; Raman spectrum, SEM and electrical characterization of the CNTs film (PDF)

Video of the surfactant driving the clip to move (AVI)

Video of the porous sponge driving the clip to move (AVI)

Video of the porous sponge driving the compression of the CNTs films (AVI)

■ AUTHOR INFORMATION

Corresponding Authors

*E-mail: tao.chen@nimte.ac.cn.

DOI: 10.1021/acs.chemmater.6b03420
Chem. Mater. 2016, 28, 7125−7133

*E-mail: zhangjiawei@nimte.ac.cn.

Notes

The authors declare no competing financial interest.

■ ACKNOWLEDGMENTS

We thank the Natural Science Foundation of China (51573203, 51303195), the Bureau of Frontier Science and Education of Chinese Academy of Sciences (QYZDB-SSW-SLH036), Young Taiwan Scholar Visiting Programme (2016TW1GA0003), Excellent Youth Foundation of Zhejiang Province of China (LR14B040001), Ningbo Science and Technology Bureau (2014B82010, 2015C110031), and Youth Innovation Promotion Association of Chinese Academy of Science (2016268).

■ REFERENCES

(1) Iijima, S.; Ichihashi, T. Single-Shell Carbon Nanotubes of 1-nm Diameter. *Nature* **1993**, *364*, 737.
(2) Hu, L.; Hecht, D. S.; Gruener, G. Carbon Nanotube Thin Films: Fabrication, Properties, and Applications. *Chem. Rev.* **2010**, *110*, 5790−5844.
(3) Wu, Z. C.; Chen, Z. H.; Du, X.; Logan, J. M.; Sippel, J.; Nikolou, M.; Kamaras, K.; Reynolds, J. R.; Tanner, D. B.; Hebard, A. F.; Rinzler, A. G. Transparent, conductive carbon nanotube films. *Science* **2004**, *305*, 1273−1276.
(4) Zhang, M.; Fang, S. L.; Zakhidov, A. A.; Lee, S. B.; Aliev, A. E.; Williams, C. D.; Atkinson, K. R.; Baughman, R. H. Strong, transparent, multifunctional, carbon nanotube sheets. *Science* **2005**, *309*, 1215−1219.
(5) Ma, W.; Song, L.; Yang, R.; Zhang, T.; Zhao, Y.; Sun, L.; Ren, Y.; Liu, D.; Liu, L.; Shen, J.; Zhang, Z.; Xiang, Y.; Zhou, W.; Xie, S. Directly synthesized strong, highly conducting, transparent single-walled carbon nanotube films. *Nano Lett.* **2007**, *7*, 2307−2311.
(6) Xiao, L.; Chen, Z.; Feng, C.; Liu, L.; Bai, Z.-Q.; Wang, Y.; Qian, L.; Zhang, Y.; Li, Q.; Jiang, K.; Fan, S. Flexible, Stretchable, Transparent Carbon Nanotube Thin Film Loudspeakers. *Nano Lett.* **2008**, *8*, 4539−4545.
(7) Cao, Q.; Rogers, J. A. Ultrathin Films of Single-Walled Carbon Nanotubes for Electronics and Sensors: A Review of Fundamental and Applied Aspects. *Adv. Mater.* **2009**, *21*, 29−53.
(8) Liu, Q. F.; Fujigaya, T.; Cheng, H. M.; Nakashima, N. Free-Standing Highly Conductive Transparent Ultrathin Single-Walled Carbon Nanotube Films. *J. Am. Chem. Soc.* **2010**, *132*, 16581−16586.
(9) Hammock, M. L.; Chortos, A.; Tee, B. C. K.; Tok, J. B. H.; Bao, Z. A. 25th Anniversary Article: The Evolution of Electronic Skin (E-Skin): A Brief History, Design Considerations, and Recent Progress. *Adv. Mater.* **2013**, *25*, 5997−6037.
(10) Du, J. H.; Pei, S. F.; Ma, L. P.; Cheng, H. M. 25th Anniversary Article: Carbon Nanotube- and Graphene-Based Transparent Conductive Films for Optoelectronic Devices. *Adv. Mater.* **2014**, *26*, 1958−1991.
(11) Lipomi, D. J.; Vosgueritchian, M.; Tee, B. C. K.; Hellstrom, S. L.; Lee, J. A.; Fox, C. H.; Bao, Z. Skin-like pressure and strain sensors based on transparent elastic films of carbon nanotubes. *Nat. Nanotechnol.* **2011**, *6*, 788−792.
(12) Liu, K.; Sun, Y.; Chen, L.; Feng, C.; Feng, X.; Jiang, K.; Zhao, Y.; Fan, S. Controlled growth of super-aligned carbon nanotube arrays for spinning continuous unidirectional sheets with tunable physical properties. *Nano Lett.* **2008**, *8*, 700−705.
(13) Saran, N.; Parikh, K.; Suh, D.-S.; Muñoz, E.; Kolla, H.; Manohar, S. K. Fabrication and Characterization of Thin Films of Single-Walled Carbon Nanotube Bundles on Flexible Plastic Substrates. *J. Am. Chem. Soc.* **2004**, *126*, 4462−4463.
(14) Jo, J. W.; Jung, J. W.; Lee, J. U.; Jo, W. H. Fabrication of Highly Conductive and Transparent Thin Films from Single-Walled Carbon Nanotubes Using a New Non-ionic Surfactant via Spin Coating. *ACS Nano* **2010**, *4*, 5382−5388.
(15) Wang, Y.; Angelatos, A. S.; Caruso, F. Template synthesis of nanostructured materials via layer-by-layer assembly. *Chem. Mater.* **2008**, *20*, 848−858.
(16) Olek, M.; Ostrander, J.; Jurga, S.; Mohwald, H.; Kotov, N.; Kempa, K.; Giersig, M. Layer-by-layer assembled composites from multiwall carbon nanotubes with different morphologies. *Nano Lett.* **2004**, *4*, 1889−1895.
(17) Shi, Z.; Chen, X. J.; Wang, X. W.; Zhang, T.; Jin, J. Fabrication of Superstrong Ultrathin Free-Standing Single-Walled Carbon Nanotube Films via a Wet Process. *Adv. Funct. Mater.* **2011**, *21*, 4358−4363.
(18) Wang, X. W.; Li, G. H.; Liu, R.; Ding, H. Y.; Zhang, T. Reproducible layer-by-layer exfoliation for free-standing ultrathin films of single-walled carbon nanotubes. *J. Mater. Chem.* **2012**, *22*, 21824−21827.
(19) Li, X.; Zhang, L.; Wang, X.; Shimoyama, I.; Sun, X.; Seo, W.-S.; Dai, H. Langmuir-Blodgett assembly of densely aligned single-walled carbon nanotubes from bulk materials. *J. Am. Chem. Soc.* **2007**, *129*, 4890−4891.
(20) Acharya, S.; Hill, J. P.; Ariga, K. Soft Langmuir-Blodgett Technique for Hard Nanomaterials. *Adv. Mater.* **2009**, *21*, 2959−2981.
(21) Giancane, G.; Ruland, A.; Sgobba, V.; Manno, D.; Serra, A.; Farinola, G. M.; Omar, O. H.; Guldi, D. M.; Valli, L. Aligning Single-Walled Carbon Nanotubes By Means Of Langmuir-Blodgett Film Deposition: Optical, Morphological, and Photo-electrochemical Studies. *Adv. Funct. Mater.* **2010**, *20*, 2481−2488.
(22) Zasadzinski, J. A.; Viswanathan, R.; Madsen, L.; Garnaes, J.; Schwartz, D. K. LANGMUIR-BLODGETT-FILMS. *Science* **1994**, *263*, 1726−1733.
(23) Ariga, K.; Yamauchi, Y.; Mori, T.; Hill, J. P. 25th Anniversary Article: What Can Be Done with the Langmuir-Blodgett Method? Recent Developments and its Critical Role in Materials Science. *Adv. Mater.* **2013**, *25*, 6477−6512.
(24) Ariga, K.; Hill, J. P. Monolayers at Air-Water Interfaces: From Origins-of-Life to Nanotechnology. *Chem. Rec.* **2011**, *11*, 199−211.
(25) Steenackers, M.; Gigler, A. M.; Zhang, N.; Deubel, F.; Seifert, M.; Hess, L. H.; Lim, C. H. Y. X.; Loh, K. P.; Garrido, J. A.; Jordan, R.; Stutzmann, M.; Sharp, I. D. Polymer Brushes on Graphene. *J. Am. Chem. Soc.* **2011**, *133*, 10490−10498.
(26) Zheng, Z.; Nottbohm, C. T.; Turchanin, A.; Muzik, H.; Beyer, A.; Heilemann, M.; Sauer, M.; Golzhauser, A. Janus Nanomembranes: A Generic Platform for Chemistry in Two Dimensions. *Angew. Chem., Int. Ed.* **2010**, *49*, 8493−8497.
(27) Li, X.; Yang, T.; Yang, Y.; Zhu, J.; Li, L.; Alam, F. E.; Li, X.; Wang, K.; Cheng, H.; Lin, C.-T.; Fang, Y.; Zhu, H. Large-Area Ultrathin Graphene Films by Single-Step Marangoni Self-Assembly for Highly Sensitive Strain Sensing Application. *Adv. Funct. Mater.* **2016**, *26*, 1322−1329.
(28) Cao, Q.; Han, S. J.; Tulevski, G. S.; Zhu, Y.; Lu, D. D.; Haensch, W. Arrays of single-walled carbon nanotubes with full surface coverage for high-performance electronics. *Nat. Nanotechnol.* **2013**, *8*, 180−186.
(29) Gao, P.; He, J.; Zhou, S.; Yang, X.; Li, S.; Sheng, J.; Wang, D.; Yu, T.; Ye, J.; Cui, Y. Large-Area Nanosphere Self-Assembly by a Micro-Propulsive Injection Method for High Throughput Periodic Surface Nanotexturing. *Nano Lett.* **2015**, *15*, 4591.
(30) Zhang, L.; Xiao, P.; Lu, W.; Zhang, J.; Gu, J.; Huang, Y.; Chen, T. Macroscopic Ultrathin Film as Bio-Inspired Interfacial Reactor for Fabricating 2D Freestanding Janus CNTs/AuNPs Hybrid Nanosheets with Enhanced Electrical Performance. *Adv. Mater. Interfaces* **2016**, *3*, 1600170.
(31) Wang, X.; Xiong, Z.; Liu, Z.; Zhang, T. Exfoliation at the Liquid/Air Interface to Assemble Reduced Graphene Oxide Ultrathin Films for a Flexible Noncontact Sensing Device. *Adv. Mater.* **2015**, *27*, 1370−1375.
(32) Wang, X. W.; Gu, Y.; Xiong, Z. P.; Cui, Z.; Zhang, T. Silk-Molded Flexible, Ultrasensitive, and Highly Stable Electronic Skin for Monitoring Human Physiological Signals. *Adv. Mater.* **2014**, *26*, 1336−1342.
(33) de Gennes, P.-G. Soft Matter (Nobel Lecture). *Angew. Chem., Int. Ed. Engl.* **1992**, *31*, 842−845.

DOI: 10.1021/acs.chemmater.6b03420
Chem. Mater. 2016, 28, 7125−7133

(34) Liang, F.; Zhang, C.; Yang, Z. Rational Design and Synthesis of Janus Composites. *Adv. Mater.* **2014**, *26*, 6944−6949.
(35) Zhang, L. M.; Yu, J. W.; Yang, M. M.; Xie, Q.; Peng, H. L.; Liu, Z. F. Janus graphene from asymmetric two-dimensional chemistry. *Nat. Commun.* **2013**, *4*, 1443.
(36) Xiao, P.; Wan, C.; Gu, J.; Liu, Z.; Men, Y.; Huang, Y.; Zhang, J.; Zhu, L.; Chen, T. 2D Janus Hybrid Materials of Polymer-Grafted Carbon Nanotube/Graphene Oxide Thin Film as Flexible, Miniature Electric Carpet. *Adv. Funct. Mater.* **2015**, *25*, 2428−2435.
(37) Gu, J.; Xiao, P.; Huang, Y.; Zhang, J.; Chen, T. Controlled functionalization of carbon nanotubes as superhydrophobic material for adjustable oil/water separation. *J. Mater. Chem. A* **2015**, *3*, 4124−4128.
(38) Gu, J.; Xiao, P.; Chen, J.; Zhang, J.; Huang, Y.; Chen, T. Janus Polymer/Carbon Nanotube Hybrid Membranes for Oil/Water Separation. *ACS Appl. Mater. Interfaces* **2014**, *6*, 16204−16209.
(39) Steenackers, M.; Jordan, R.; Kuller, A.; Grunze, M. Engineered Polymer Brushes by Carbon Templating. *Adv. Mater.* **2009**, *21*, 2921−2925.
(40) Stuart, M. A. C.; Huck, W. T. S.; Genzer, J.; Mueller, M.; Ober, C.; Stamm, M.; Sukhorukov, G. B.; Szleifer, I.; Tsukruk, V. V.; Urban, M.; Winnik, F.; Zauscher, S.; Luzinov, I.; Minko, S. Emerging applications of stimuli-responsive polymer materials. *Nat. Mater.* **2010**, *9*, 101−113.
(41) Chen, T.; Ferris, R.; Zhang, J.; Ducker, R.; Zauscher, S. Stimulus-responsive polymer brushes on surfaces: Transduction mechanisms and applications. *Prog. Polym. Sci.* **2010**, *35*, 94−112.
(42) Hummers, W. S.; Offeman, R. E. Prepartion of Graphitic Oxide. *J. Am. Chem. Soc.* **1958**, *80*, 1339−1339.
(43) Steenackers, M.; Kuller, A.; Stoycheva, S.; Grunze, M.; Jordan, R. Structured and Gradient Polymer Brushes from Biphenylthiol Self-Assembled Monolayers by Self-Initiated Photografting and Photopolymerization (SIPGP). *Langmuir* **2009**, *25*, 2225−2231.

DOI: 10.1021/acs.chemmater.6b03420
Chem. Mater. 2016, 28, 7125−7133